Separation Science and Technology
Publication details, including instructions for authors and subscription information:
http://www.informaworld.com/smpp/title~content=t713708471

Operation Strategies for Simulated Moving Bed in the Presence of Adsorbent Ageing

Pedro Sá Gomes[a]; Mirjana Minceva[a]; Alírio E. Rodrigues[a]
[a] Department of Chemical Engineering-Faculty of Engineering, Laboratory of Separation and Reaction Engineering (LSRE), University of Porto Rua Dr. Roberto Frias s/n, Porto, Portugal

To cite this Article Gomes, Pedro Sá , Minceva, Mirjana and Rodrigues, Alírio E.(2007) 'Operation Strategies for Simulated Moving Bed in the Presence of Adsorbent Ageing', Separation Science and Technology, 42: 16, 3555 — 3591
To link to this Article: DOI: 10.1080/01496390701710703
URL: http://dx.doi.org/10.1080/01496390701710703

Separation Science and Technology, 42: 3555–3591, 2007

ISSN 0149-6395 print/1520-5754 online
DOI: 10.1080/01496390701710703

Operation Strategies for Simulated Moving Bed in the Presence of Adsorbent Ageing

Pedro Sá Gomes, Mirjana Minceva, and Alírio E. Rodrigues
Department of Chemical Engineering-Faculty of Engineering, Laboratory of Separation and Reaction Engineering (LSRE), University of Porto Rua Dr. Roberto Frias s/n, Porto, Portugal

Abstract: The effect of adsorbent ageing on the operation of Simulated Moving Bed (SMB) units is addressed, for two different systems (linear and non-linear isotherms). Two different consequences of adsorbent deactivation are considered, one involving the loss of adsorption equilibrium capacity and the other related to the increase of mass transfer resistance. For each of these cases one direct and straightforward compensation measure is presented: the increase of the solid velocity (decrease of switching time) to compensate the adsorbent capacity decline and the decrease of solid and internal flow rates to compensate the mass transfer resistances increase. It is possible to compensate the adsorbent capacity decline, maintaining all SMB performance parameters, limited to the reduced contact time when high solid velocities are used. In the second case, when mass transfer resistance increases, it has been shown that the direct compensation strategy would lead to a decrease of productivity, to keep the same purity and recovery as with fresh adsorbent.

Another possible corrective method to the ageing problem is the use of variable switching times in the non-conventional *"modus operandi"*-Varicol, a sort of re-arrangement of the SMB columns distribution by sections, here tested for the case of adsorbent capacity decline case as a consequence of adsorbent ageing mechanisms.

Keywords: Simulated moving bed, true moving bed, ageing, deactivation, adsorption, separation

Received 3 May 2007, Accepted 5 September 2007
Address correspondence to Alírio E. Rodrigues, Department of Chemical Engineering-Faculty of Engineering, Laboratory of Separation and Reaction Engineering (LSRE), University of Porto Rua Dr. Roberto Frias s/n, Porto, Portugal. E-mail: arodrig@fe.up.pt

INTRODUCTION

The Simulated Moving Bed (SMB) technology patented by Brougthon and Gerhold (1), is an inventive solution for the True Moving Bed (TMB) operating problems related to the solid motion. Contrary to the TMB units, where the solid phase moves counter currently to the fluid phase, in the SMB units the solid motion is simulated by a synchronous shift of all inlet and outlet ports, while the solid phase is held immobile. The SMB technology has been mainly applied to the so-called "difficult separations," in fields such as the petrochemical area with the separation of *p*-xylene from C_8 isomers mixtures (Parex process from UOP (2) or the Eluxyl process from IFP (3, 4)). The expansion of new SMB applications in fields such as the biotechnological, fine chemistry, and pharmaceutical industries has been remarkable in the last decade (5, 6).

All this interest in the SMB technology resulted in a considerable number of publications concerning the development of mathematical models and simulation methods, design techniques and optimization approaches, experimental studies, and analyses of various processes, in view of the design and construction of high performance SMB units. Also, some non-conventional SMB modes of operation have been presented, as for example the Varicol (7, 8) considering an asynchronous ports shift, the PowerFeed (9) and Modicon (10, 11) for variable flow rate or variable feed concentration respectively, OSS (Outlet Streams Swing) the periodical collection on the outlet ports (12), the MultiFeed (12, 13), semicontinuous two-zone SMB/chromatography (14, 15), the pseudo-SMB (Japan Organo-tech) (16, 17) for multicomponent separations operating at 2 different steps, SMBR (SMB with reaction) as for the diethylacetal production (18, 19). All the work developed around the SMB technology has shown the importance of this chromatographic separation technique in a wide range of applications.

Adsorbent/Catalyst deactivation (or ageing) has been the subject of several studies in the reactive/separation engineering field. The Adsorbent/Catalyst ageing mechanisms are generally divided into six groups (20):

i. Poisoning, caused by irreversible or "pseudo-irreversible" adsorption of some species in the adsorbent active sites;
ii. Fouling, physical (mechanical) deposition of species from the fluid phase onto the solid one, resulting in activity losses due to sites and/or pores obstruction;
iii. Thermally-induced deactivation (sintering, etc. . .);
iv. Vapor compound formation accompanied by transport;
v. Vapor-solid and/or solid-solid reactions;
vi. Attrition/Crushing, mechanical failure (quite usual in moving bed and fluidized-bed systems).

Literature addressing the catalyst/adsorbent deactivation and possible solutions has been published and expanded considerably over the past three

decades: review articles (21–24) books (25–28) and proceedings of international symposia (29–34).

Nevertheless, regarding the Simulated Moving Bed (SMB) technology, the work published on catalyst/adsorbent ageing is almost nonexistent as reported elsewhere (35, 36). The information considering this issue remains restricted to the plant operators and technology owners and mainly particle size re-distribution and capacity decline are mentioned as a result of adsorbent ageing leading to process performance decrease.

It is from the common wisdom of the use of guard beds, as in the gas processing industry, avoiding impurities to enter in the separation process (37). Nevertheless, ageing problems such as secondary/parallel reactions with the solid phase or liquid phase, attrition, leading to fine and channelling etc. cannot be handled by using guard beds.

By treating adsorbent ageing as a disturbance it is possible to compensate it by applying SMB online controllers as pointed out by Engell or Morari research groups (38–41). However, the implementation of the model predictive control methods should also be based on ageing models as compensative measures.

Modelling-based research is required to define the ageing problem consequences and indicate strategies that can be used to mitigate capacity loss or other deactivation effects (42). The current practice in industrial chiral separations involves the replacement of 10% of adsorbent fines (which results from pressure fluctuations) after one year of operation and repacking of columns. Recently more elaborated methods such as online adsorbent removal (43, 44) and innovative fluid distribution apparatus (45) are used.

Time scales of catalyst/adsorbent deactivation vary in a wide range from few seconds in the case of catalyst cracking, up to 5 to 10 years, as for example in ammonia synthesis with iron catalyst (20). In SMBs separations the adsorbent decline also takes place in different time scales. Rapid perturbations involving dramatic changes on the inlet concentrations, for example, the entrance of heavy impurities result on considerable ageing problems, but it is not the purpose of this work to address these unpredicted aspects. However, chiral separations are known to work at reasonable efficiency just for 3 to 5 years while in *p*-xylene separation a 20–30% adsorbent capacity decline occurs during a 10 to 20 years period (36). These are slow mechanisms, when compared to the dynamic characteristics of the SMB process (the dynamics of attainment of the unit cyclic steady state after some perturbation), but common in the operation of almost SMB units, and therefore, the ones analysed in detail on this work.

A productive SMB unit depends on the calculation of optimal operating parameters (ratio between fluid and the simulated solid interstitial velocities) obtained from the so-called separation region, a feasible region that represents all points that will provide the required separation performance, usually with a triangular shape. The optimal unit performance is obtained when working near the vertex of this "triangle," and therefore a slight change in the operating

point will lead to the violation of one or more of the separation conditions ruining all the operation (46). This slight movement of the operating point could result from the adsorbent ageing problem, even if the operating parameters (internal flows, columns arrangements etc.), are kept at constant values as the ones calculated for the initial unit design.

The idea of working near the best operation point (near to the vertex and to the Lower Solvent Consumption point), and adjust this location with the adsorbent deactivation, trying to keep it at the same relative distance, is attractive as an adsorbent ageing corrective action. In addition, it is widely accepted nowadays that process innovation is based not only on the challenges, problems, and needs but also on the social, political, and cultural conditions prevailing in the prospective market.

Therefore, the objective of this work is to study the effect of adsorbent ageing on the performance parameters of an SMB unit and to propose some operating strategies to overcome this problem. The same methodology, can also be applied to the comparison of adsorbent with different properties as the tuning of SMB units after complete/partial change in the adsorbent, with fresh or improved adsorbent.

Two different consequences of the above-stated adsorbent deactivation mechanisms are considered in this study: the adsorbent capacity decrease and the increase of mass transfer resistances. For each case different strategies are presented:

i. the decrease of switching time (solid flow rate increase), as a continuous corrective strategy for the adsorbent capacity decrease; and
ii. the decrease of internal flow rates and increase of switching time to compensate the mass transfer resistances increase.

The compensation strategies are not similar or compatible and therefore it is important to understand which is the most significant cause for adsorbent deactivation (the solid capacity decrease or the mass transfer resistances increase). A simple diagnosis method is also suggested to simplify this task.

Also, a non-continuous strategy is presented: the unit rearrangement, and different number of columns per section with the ageing evolution. These corrective operational strategies of adsorbent ageing could lead to the extension of the sieve life, keeping similar performance parameters (productivity, recovery, and product purities), as the ones established with the initial SMB unit design.

MODELLING AND DESIGN STRATEGIES

As already mentioned the SMB operation mode (Fig. 1 (a)) is a practical implementation of the continuous counter current TMB process (Fig. 1 (b)), and the equivalence between TMB and an hypothetical infinite column number SMB is usually explored in the modelling field.

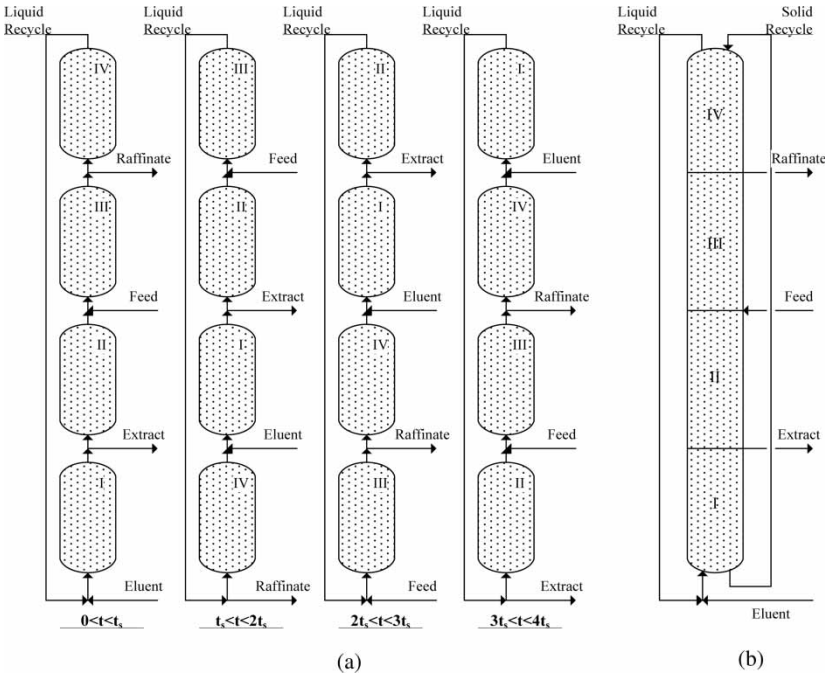

Figure 1. Schematic representation of a 4 columns SMB unit operating over a complete cycle (a), from 0 to $4t_s$ (with t_s representing the ports switching time) and the equivalent "4 columns length" TMB unit (b).

In the SMB unit (or equivalent TMB), it is possible to define 4 different zones/sections, each of one placed between one inlet and one outlet port. The solid regeneration zone (zone 1) is placed between the eluent and extract ports and the eluent regeneration zone (zone 4) between the raffinate and eluent ports. The separation zones are limited by the extract and feed ports (zone 2) and feed and raffinate ports (zone 3), as shown in Fig. 1. The equivalence between the SMB model and the TMB model is established through the relation between the SMB liquid phase interstitial velocity (u_j^*), the TMB liquid (u_j) and solid (u_s) interstitial velocity in each section j : $u_j^* = u_j + u_s$. The interstitial solid velocity in the TMB, the ratio of the solid volumetric flow-rate to column cross section area available to the solid flow, is calculated as the ratio between the column length (L_c) and the switching time interval (t_s) in the SMB: $u_s = (L_c)/t_s$. Therefore, the internal flow-rates in both models are not the same, but related by $Q_j^* = Q_j + (\varepsilon_b\, V_c)/(t_s)$, where Q_j^* and Q_j are the internal liquid flow-rates in the SMB unit and TMB model, respectively, V_c is the column volume and ε_b is the bed porosity.

In this work, both SMB and TMB modelling strategies are used to study the influence of adsorbent ageing on the SMB performance and to simulate the

effect of the theoretical adsorbent ageing corrective measures. The simulations of the bulk concentration profiles for selected case studies are always performed only with the SMB model. The TMB methodology saves computer time, providing acceptable results when modelling units with higher number of columns per section.

TMB Design and Operating Parameters

The design of a TMB unit consists of the adjustment of flow rates in each zone in a way that the less retained component (B) would be recovered in the raffinate and the more retained one (A) in the extract, avoiding the contamination of the raffinate stream with the more retained species and presence of less retained one in the extract stream. To achieve these separation objectives the following constraints of the species net fluxes in each section, here described in terms of the dimensionless γ_j operating parameters, should be established,

$$\gamma_1 > \frac{1-\varepsilon_b}{\varepsilon_b}\frac{\langle q_{A1}\rangle}{C_{bA1}} \tag{1a}$$

$$\frac{1-\varepsilon_b}{\varepsilon_b}\frac{\langle q_{B2}\rangle}{C_{bB2}} < \gamma_2 < \frac{1-\varepsilon_b}{\varepsilon_b}\frac{\langle q_{A2}\rangle}{C_{bA2}} \tag{1b}$$

$$\frac{1-\varepsilon_b}{\varepsilon_b}\frac{\langle q_{B3}\rangle}{C_{bB3}} < \gamma_3 < \frac{1-\varepsilon_b}{\varepsilon_b}\frac{\langle q_{A3}\rangle}{C_{bA3}} \tag{1c}$$

$$\gamma_4 < \frac{1-\varepsilon_b}{\varepsilon_b}\frac{\langle q_{B4}\rangle}{C_{bB4}} \tag{1d}$$

where C_{bij} represents the bulk fluid phase concentration of species i in section j, $\langle q_{ij}\rangle$ the average solid concentration of species i in section j and γ_j the ratio between the TMB fluid and solid interstitial velocities in section j.

The γ_j parameters are similar to the m_j from Morbidelli's group (47), which represents the ratio of flow rates of the fluid and solid phases.

In absence of mass transfer limitation, the Equilibrium Theory (48–53) which assumes that the adsorption equilibrium is established everywhere at any time, can be applied to the TMB model equations, resulting in a feasible region (separation region) formed by the constraints (1b) and (1c), well known as the Triangle Theory (47, 54, 55). The separation region presented in the ($\gamma_2 \times \gamma_3$) plane is a rectangular triangle for linear adsorption isotherms cases or a triangular shaped form for non linear isotherms cases. Figure 2 represents the separation region and regeneration zones for the linear adsorption isotherms case (case study from Leão and Rodrigues (56)), where the separation triangle upper limit is defined by $(1-\varepsilon_b)/(\varepsilon_b)K_A$, and the lower limit by $(1-\varepsilon_b)/(\varepsilon_b)K_B$, while for the regeneration zones the γ_1 lower limit is $(1-\varepsilon_b)/(\varepsilon_b)K_A$and the γ_4 upper limit is

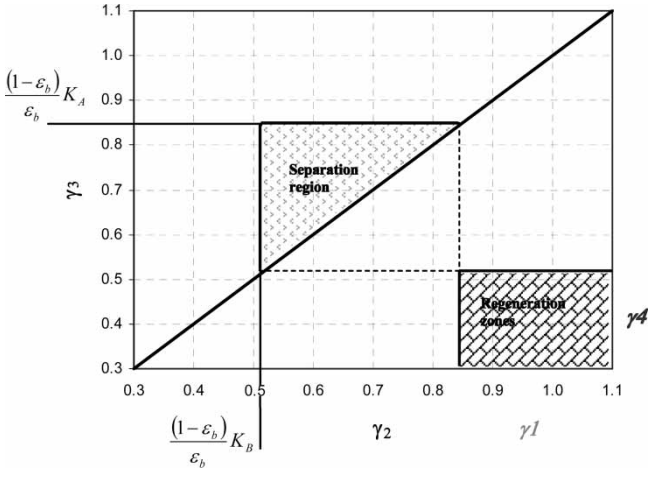

Figure 2. Triangle theory applied to the design of an TMB unit: constraints for the separation region and regeneration zones.

$(1 - \varepsilon_b)/(\varepsilon_b)K_B$. The K_i is the species i Henry constant for the linear adsorption isotherms here considered.

The TMB and SMB models consider a convective fluid flow with axial dispersion, counter current solid plug flow (in the case of TMB), negligible thermal effects, constant values for the bed void fraction ε_b, particle radius R_p, axial dispersion coefficient D_{bj}, particle effective diffusivity D_{pe} and film mass transfer coefficient k_f; diluted solutions and therefore constant values for the flow rates/interstitial velocities in each section, and also negligible pressure drop.

Modelling of an TMB in Presence of Mass Transfer

It is possible to simulate an TMB model using a more complete model, detailing the particle diffusion and/or film mass transfer as stated for reactive systems (57). However, in this work the Linear Driving Force (LDF) concept (58), will be applied; it is an approximation to the intraparticle mass transfer, averaging the intraparticle concentration.

The TMB model nodes balances,

$$\text{Eluent node}: C_{bi(4,x=1)} = \frac{u_1}{u_4} C_{bi(1,x=0)} \tag{2a}$$

$$\text{Extract } (j = 2) \text{ and Raffinate } (j = 4) \text{ nodes}: C_{bi(j-1,x=1)} = C_{bi(j,x=0)} \tag{2b}$$

$$\text{Feed node}: C_{bi(2,x=1)} = \frac{u_3}{u_2} C_{bi(3,x=0)} - \frac{u_F}{u_2} C_i^F \tag{2c}$$

and,

$$u_1 = u_4 + u_E \quad \text{Eluent(E) node;} \tag{3a}$$
$$u_2 = u_1 - u_X \quad \text{Extract(X) node;} \tag{3b}$$
$$u_3 = u_2 + u_F \quad \text{Feed(F) node;} \tag{3c}$$
$$u_4 = u_3 - u_R \quad \text{Raffinate(R) node.} \tag{3d}$$

The species mass balances are:
for the bulk fluid:

$$\frac{\partial C_{bij}}{\partial \theta} = \frac{\gamma_j}{n_j}\left\{\frac{1}{Pe_j}\frac{\partial^2 C_{bij}}{\partial x^2} - \frac{\partial C_{bij}}{\partial x} - \frac{(1-\varepsilon_b)}{\varepsilon_b}\alpha_{ij}(q^*_{ij} - \langle q_{ij}\rangle)\right\} \tag{4}$$

and for "solid phase":

$$\frac{\partial \langle q_{ij}\rangle}{\partial \theta} = \frac{1}{n_j}\frac{\partial \langle q_{ij}\rangle}{\partial x} + \frac{\gamma_j}{n_j}\alpha_{ij}(q^*_{ij} - \langle q_{ij}\rangle) \tag{5}$$

with the initial and boundary conditions,

$$\begin{cases} C_{bij}(x,0) = 0; \\ \langle q_{ij}(x,0)\rangle = 0; \end{cases} \tag{6}$$

$$x = 0\colon C_{bi(j,x=0)} = C_{bij}(0,\theta) - \frac{1}{Pe_j}\left.\frac{\partial C_{bij}}{\partial x}\right|_{x=0} \tag{7}$$

$$x = 1\colon \left.\frac{\partial C_{bij}}{\partial x}\right|_{x=1} = 0 \tag{8}$$

and

$$x = 1\begin{cases} \langle q_{ij}\rangle = \langle q_{i(j+1,x=0)}\rangle, & \text{for } j = 1,2,3; \\ \langle q_{i4}\rangle = \langle q_{i(1,x=0)}\rangle \end{cases} \tag{9}$$

and the adsorption equilibrium isotherm defined as:

$$q^*_{ij} = f_i(C_{bij}, C_{bkj}) \text{ with} k \neq i \text{ and for all species } i \text{ and in section } j \tag{10}$$

where C_i^F is the species i feed inlet concentration, $\theta = (t)/(t_s)$ is the dimensionless time normalised by the SMB ports switching time t_s, $x = (z)/(L_j)$ is the dimensionless axial coordinate with respect to $L_j = L_c n_j$ is the j section length, $\gamma_j = (u_j)/(u_s)$ is the ratio between fluid and solid interstitial velocities, $Pe_j = (u_j L_j)/(D_{bj})$ is the section j Peclet number, $t_j = (L_j)/(u_j)$ is the fluid phase space time, and $\alpha_{ij} = k_{LDF} \cdot t_j$.

Modelling of an SMB in Presence of Mass Transfer

In the case of reduced number of columns a more realistic SMB model should be applied, where after each switch interval the boundary conditions for each column are synchronously changed, and therefore respecting always the nodes mass balances,

$$\text{Eluent node: } C_{bi(4,x^*=1)} = \frac{u_1^*}{u_4^*} C_{bi(1,x^*=0)} \tag{11a}$$

$$\text{Extract } (j = 2) \text{ and Raffinate } (j = 4)\text{nodes: } C_{bi(j-1,x^*=1)} = C_{bi(j,x^*=0)} \tag{11b}$$

$$\text{Feed node: } C_{bi(2,x^*=1)} \frac{u_3^*}{u_2^*} C_{bi(3,x^*=0)} - \frac{u_F}{u_2^*} C_i^F \tag{11c}$$

where,

$$u_1^* = u_4^* + u_E \quad \text{Eluent(E) node;} \tag{12a}$$

$$u_2^* = u_1^* - u_X \quad \text{Extract(X) node;} \tag{12b}$$

$$u_3^* = u_2^* + u_F \quad \text{Feed(F) node;} \tag{12c}$$

$$u_4^* = u_3^* - u_R \quad \text{Raffinate(R) node;} \tag{12d}$$

with u_j^* representing the fluid interstitial velocity in section j of the SMB equipment. This time-dependence of the boundary conditions for each column in each section j leads to a cyclic steady-state (CSS), instead of the real steady-state achieved for the true moving bed (TMB).

Transient mass balances for each species i in each column c, of section j, are:
in the bulk fluid phase,

$$\frac{\partial C_{bic}}{\partial \theta} = \gamma_j^* \left\{ \frac{1}{Pe_c^*} \frac{\partial^2 C_{bic}}{\partial x^{*2}} - \frac{\partial C_{bic}}{\partial x^*} \right\} - \frac{(1 - \varepsilon_b)}{\varepsilon_b} \alpha_{ic}^* (q_{ic}^* - \langle q_{ic} \rangle) \tag{13}$$

and in the bed "solid-phase",

$$\frac{\partial \langle q_{ic} \rangle}{\partial \theta} = \alpha_{ic}^* (q_{ic}^* - \langle q_{ic} \rangle) \tag{14}$$

The initial and boundary conditions are:

$$\begin{cases} C_{ic}(x^*, 0) = 0; \\ \langle q_{ic}(x^*, 0)\rangle = 0; \end{cases} \tag{15}$$

$$x^* = 0 : C_{bic}(0^-, \theta) = C_{bic}(0, \theta) - \frac{1}{Pe_c^*}\frac{\partial C_{bic}}{\partial x^*}\bigg|_{x^*=0}, c = 1 \text{ to } Nc \tag{16}$$

$$x^* = 1 : \frac{\partial C_{bic}}{\partial x}\bigg|_{x^*=1} = 0 \tag{17}$$

and the adsorption equilibrium isotherm is defined by Eq. (10).

In the above model equations $C_{bic}(0^-, \theta)$ represents the inlet concentration of species i in column c, $x^* = (z)/(L_c)$, $\gamma_j^* = (u_j^*)/u_s$) (ratio between SMB fluid and equivalent solid interstitial velocities), $Pe_c^* = (u_j^* L_c)/(D_{bj})$ is the Peclet number, and $\alpha_{ic}^* = k_{LDF} \cdot t_s$ is the number of intraparticle mass transfer units in the SMB model.

Alternatively all mass transfer resistances and axial dispersion effects can be included in a pseudo-LDF equivalent number of intraparticle mass transfer units (59),

$$\frac{1}{k_{LDF}K_i} = \frac{D_{bj}}{u_j^2}\left(\frac{1-\varepsilon_b}{\varepsilon_b}\right) + \frac{R_p}{3k_f} + \frac{R_p^2}{15D_{pe}K_i} \tag{18}$$

For SMB a global k_{LDF}^* based on u_j^* should be used.

Equation (18) results from the equivalence of the model represented by Eqs. (4) and (5) (or 13 and 14), and a simpler one which considered plug flow for the fluid phase and lumped all kinetic effects in a pseudo-LDF parameter (k_{LDF} or k_{LDF}^*). This is an extension of the Glueckauf approximation for linear systems in which more than one mass transfer resistance and axial dispersion are significant and based on the equality of moments of impulse responses for both models. The term $(1)/(Pe_j)\ (\partial^2 C_{bij})/(\partial x^2)$ in Eq. (4) or $(1)/(Pe_c^*)\ (\partial^2 C_{bic})/(\partial\, x^{*2})$ in Eq. (13) is then neglected, since the axial dispersion contribution is already considered in Eq. (18).

Performance Parameters

The SMB outlet/inlet flow rates must satisfy purity and recovery specifications, the so-called performance parameters. The definitions of extract purity (*PUX*, %), raffinate purity (*PUR*, %), recovery *i* species in the extract current (*REX*, %), recovery of the *i* species in the raffinate (*RER*, %), and the unit productivity in terms of A in the extract (PR_X^A) or *B* species in raffinate (PR_R^B), that characterize each SMB unit performance, operating at

certain conditions for the SMB model at cyclic steady state, are given below,

$$PUX^i = 100(\%)\frac{\int_\theta^{\theta+1} C_{bi}^X d\theta}{\sum_{k=1}^{NC}\int_\theta^{\theta+1} C_{bk}^X d\theta} \tag{19a}$$

$$REX^i = 100(\%)\frac{Q_X\int_\theta^{\theta+1} C_{bi}^X d\theta}{Q_F\int_\theta^{\theta+1} C_i^F d\theta} \tag{19b}$$

$$PR_X^i = \frac{Q_X\int_\theta^{\theta+1} C_{bi}^X d\theta}{V_{bed}(1-\varepsilon_b)} = \frac{REX^i \cdot Q_F\int_\theta^{\theta+1} C_i^F d\theta}{V_{bed}(1-\varepsilon_b)} \tag{19c}$$

where Q_X and Q_F are the extract and feed flow rates respectively, and V_{bed} the adsorbent volume. Similar definitions hold for purity, recovery and productivity of the raffinate.

Numerical Solution Strategy

The TMB and SMB model equations were numerically solved using the gPROMS v3.0.2 a commercial package from Process Systems Enterprise, (www.psenterprise.com). The mathematical models, composed by systems of PDE (Partial Differential Equations), ODE (Ordinary Differential Equations) and AE (Algebraic Equations), were solved using the discretization methods available in gPROMS. The PDE were discretized in axial direction using OCFEM (Orthogonal Collocation on Finite Elements) method, with 2 collocation points per element and 100 elements per each zone/section. After the axial discretization step, the time integration of the ODEs system is performed using the variable time step SRADAU solver, a fully-implicit Runge-Kutta method. Finally, the resulting system of equations is then solved with the gPROMS BDNSOL (Block decomposition NonLinear SOLver).

It is assumed that an SMB simulation has reached the CSS, when the columns profiles in two consecutive cycles have less than 1.0% of relative deviation, the global mass balance is verified with less than 1.0% of relative error, the global numeric error between iterations being lower than 10^{-5}.

ADSORBENT AGEING PROBLEM

Adsorbent/catalyst deactivation is generally the result of a number of unwanted chemical and physical changes (20). The causes of deactivation can be divided in three major categories: chemical, thermal, and mechanical. In this work the thermal effects, generally associated with high amplitude changes of the operating temperature, will not be considered.

The mechanical deactivation, as a result of physical breakage, attrition, or crushing of the adsorbent particle is an important deactivation phenomenon in the SMB separation field. Associated with particle size changes during the SMB unit operation are the increased columns packing heterogeneity, the formation of preferential paths (channelling), the stagnant zones problems, the increase of pressure drop and dispersion, which lead to substantial drop of columns efficiency. Nevertheless, in terms of consequences, the establishment of preferential paths or dead volumes can be associated with a "global adsorbent capacity" decline (and treated as adsorbent capacity decline), and particle size redistribution associated with the LDF mass transfer coefficient.

Chemical and mechanical deactivation mechanisms may affect both the adsorbent capacity and the intraparticle kinetics. Therefore, instead of studying each adsorbent ageing mechanism separately, the definition of compensation strategies for the two major consequences of the adsorbent deactivation (loss of adsorbent capacity or increase of the mass transfer resistances), is taken as the principal objective to this work. First of all it would be needed to observe the impact of both the adsorbent deactivation consequences on the operation of a regular SMB unit. Secondly, on the basis of the conclusions from these studies, some compensation procedures to overcome ageing problems would be proposed.

Adsorbent Capacity Decline Due to Adsorbent Deactivation

Under the assumption of the Equilibrium Theory, in Fig. 2 it can be noted that each SMB design problem is based on the adsorption isotherms. The adsorbent deactivation considered here is only the adsorption capacity decline; it will change the adsorption equilibrium isotherms and therefore the whole design problem. To maintain the same or similar SMB performance parameters it would be needed to recalculate new operating parameters. In this way, it is important to study the influence of the adsorbent capacity decline on the separation triangle region, and the rectangular regeneration zones shape (see Fig. 2), in order to formulate corrective strategies for the operating parameters to overcome the ageing problem and to maintain the SMB performance parameters the closest possible to the initial ones.

Linear Isotherms Case

Considering a linear isotherm as general case presented with Eq. (20),

$$q_i^* = K_i C_{bi} \tag{20}$$

it can be assumed that for a constant feed concentration, the adsorbed capacity decline due to the adsorbent ageing mechanisms, can be represented by the decrease of the value of Henry's adsorption isotherm constant K_i, as

represented by Eq. (21):

$$K_i = K_i^0 \cdot f(t) \tag{21}$$

where K_i^0 represents the initial value of the Henry's adsorption isotherm constant and $f(t)$ is a general law of the adsorbent ageing as a function of time.

With the adsorbent capacity decline due to ageing problems, for binary adsorption three general scenarios can happen:

i. the deactivation is the same for the different species;
ii. it is higher for the more adsorbed species;
iii. it is higher for the less adsorbed species.

For one species deactivation cases (ii or iii), it is simple to see how the separation zone triangle will be reduced by the upper limit $((1 - \varepsilon_b)/(\varepsilon_b)K_A)$ due to the decrease of K_A value, if the case is species A deactivation only, or will augment by the lower limit $((1 - \varepsilon_b)/(\varepsilon_b)K_B)$ due to the decrease of K_B value, if there is only B species deactivation. These cases are quite specific and almost theoretical, since the more common ageing problems are consequence from adsorbent deactivation of both species. Therefore, in this study only the case (i) will be considered, where both species have the same deactivation rates. In this case, the decrease of adsorbent capacity for both species results in migration of the separation zone downwards to lower values of γ_2 and γ_3, well represented by the change of the vertex point position, where $(\gamma_2, \gamma_3) = ((1 - \varepsilon_b)/(\varepsilon_b)K_B, (1 - \varepsilon_b)/(\varepsilon_b)K_A)$, as shown in Fig. 3.

A classic SMB binary separation with linear adsorption isotherms, as the one presented by Leão and Rodrigues (56) for the separation of a mixture with Fructose (A) and Glucose (B), characterized by the model parameters and optimized operating conditions presented in Table 1 and 2, is considered.

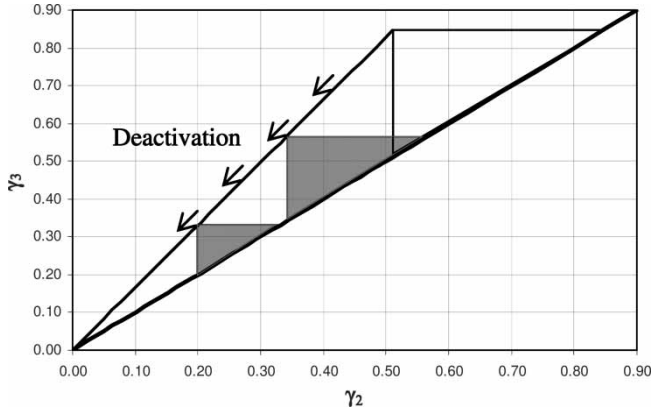

Figure 3. Triangle theory applied to an TMB design problem: new adsorbent (black) and the capacity decline effect due to aged adsorbent (gray), considering the case (i).

Table 1. SMB unit characteristic parameters (56)

Model parameters	SMB columns
$Pe = 2000$	$N_c = 12$ [3 3 3 3]
$\varepsilon_b = 0.4$;	$L_c = 11.5$ cm
	$d_c = 2.6$ cm
	SMB operating conditions
$k_{LDF} = 0.1\ s^{-1}$	$C_A^F = 30\ g.l^{-1}$; $C_B^F = 30\ g\ .\ 1^{-1}$ $t_s = 105$ s; $Q_E = 8.23\ ml \cdot min^{-1}$; $Q_X = 5.62\ ml \cdot min^{-1}$; $Q_F = 1.28\ ml \cdot min^{-1}$; $Q_R = 3.89\ ml \cdot min^{-1}$; $Q_4 = 19.89\ ml \cdot min^{-1}$

In this case study, the film mass transfer coefficient was considered to be negligible, and all mass transfer resistances for both species are represented by the k_{LDF} calculated according Eq. (18).

The linear isotherms are:

$$q_A^* = 0.5634 C_{bA} \tag{22a}$$

$$q_B^* = 0.3401 C_{bB} \tag{22b}$$

Let us assume various levels of adsorbent ageing, by reducing the Henry constant for both fructose and glucose by 2, 4, 6, and 8%, and keeping the same operating conditions as those presented in Tables 1 and 2. The internal concentration profiles at half switching time in the CSS and SMB performances at different levels of adsorbent deactivation (percentage of adsorbent capacity lost) are presented in Fig. 4 and Table 3, respectively.

As can be observed in Fig. 4 the tendency of concentration profiles change is not the same in each section, even if the adsorbent capacity decline is the same for both species. With the adsorbent capacity decline the bulk concentration fronts moved from left to the right. It is also interesting to observe that when the solute is essentially "moving" with the solid (section 4 to section 1 direction) in zones 3 and 4, the liquid bulk concentration have increased, while when the solute is being transported by the fluid phase (zone 1 and 2) the liquid bulk concentration have decreased. This tendency is noted both in the plateaus zone (zone 2 and 3) and in the regeneration zones 1 and 4. This behavior is a result of the distance between the

Table 2. The SMB and equivalent TMB section operating conditions (56)

Real SMB	Equivalent TMB
$\gamma_j^* =$[2.0149 1.6122 1.7039 1.4252]	$\gamma_j =$ [1.0149 0.6122 0.7039 0.4252]
$Q_j^* =$ [28.12 22.50 23.78 19.89] $ml \cdot min^{-1}$	$Q_j =$ [14.16 8.54 9.82 5.93] $ml \cdot min^{-1}$

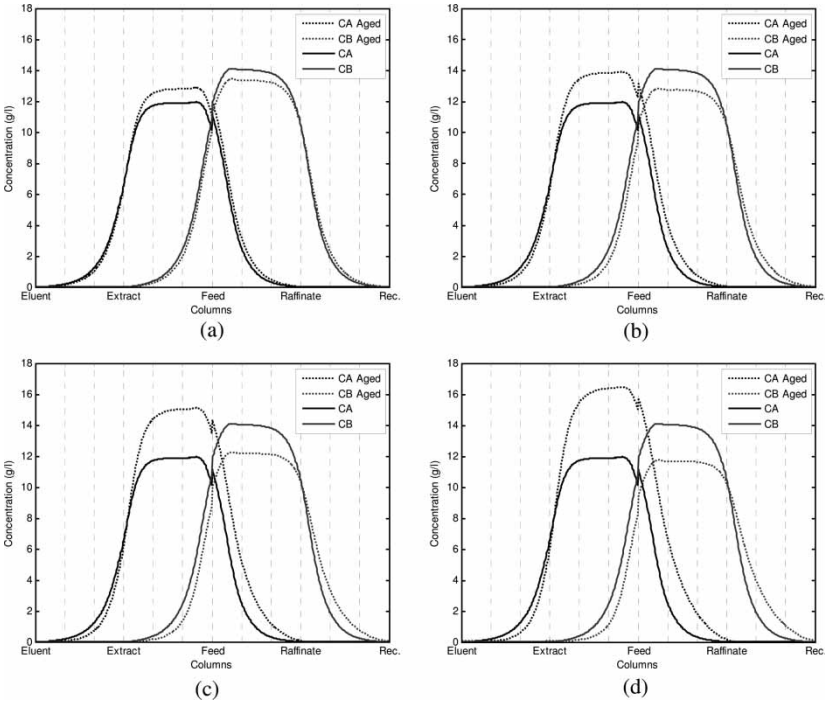

Figure 4. SMB concentration profiles of fructose (A) and glucose (B) as result of adsorbent capacity decline (a) $K_A = 0.5521$ and $K_B = 0.3333$ (less 2%), (b) $K_A = 0.5409$ and $K_B = 0.3265$ (less 4%), (c) $K_A = 0.5296$ and $K_B = 0.3197$ (less 6%) and (d) $K_A = 0.5183$ and $K_B = 0.3129$ (less 8%), at half time switch in the CSS.

operating point (represented by the set (γ_2,γ_3) and (γ_1,γ_4)) to the respective zone constraints, which changed as a result of adsorbent capacity decline.

Also, from Table 3 it can be noted that increasing the deactivation level the raffinate became more polluted than the extract; as a consequence of the fronts movement from left to right, as shown in Fig. 4.

Table 3. SMB performance parameters values for different levels of adsorbent deactivation: 2, 4, 6 and 8% (adsorbent capacity decrease: $K_A = 0.5521$ and $K_B = 0.3333$, $K_A = 0.5409$ and $K_B = 0.3265$, $K_A = 0.5296$ and $K_B = 0.3197$ and $K_A = 0.5183$ and $K_B = 0.3129$, respectively)

Deactivation (%)	PUX^A (%)	PUR^B (%)	REX^A (%)	RER^B (%)
0	99.5	99.6	99.6	99.5
2	99.6	99.5	99.5	99.6
4	99.5	99.2	99.2	99.5
6	99.4	98.7	98.7	99.4
8	99.2	97.7	97.7	99.2

It can be noticed that the concentration plateau for the more adsorbed species (A) in zone 2 was lower than that of the less adsorbed one (B) in zone 3, but at a certain adsorbent the capacity decline the level of the concentration plateaus ratio was reversed, becoming the A plateau in zone 2 higher than the B plateau in zone 3.

This behavior can be justified by the following analysis based on the equilibrium theory and using the TMB model. For the case where all A product fed to the SMB unit is recovered in the extract and all product B is recovered in the raffinate, species A will be present only in zone 2 and species B in zone 3, the solid flow in each zone is in equilibrium with the corresponding fluid flow, we get:

$$\begin{cases} Q_S K_A C_{bA2} - Q_2 C_{bA2} = Q_X C_{bAX} = Q_F C_{bAF} \\ Q_3 C_{bB3} - Q_S K_B C_{bB3} = Q_R C_{bBR} = Q_F C_{bBF} \end{cases} \quad \text{(23 a and b)}$$

or:

$$\frac{C_{bA2}}{C_{bB3}} = \frac{C_{bAF}}{C_{bBF}} \frac{Q_3 - Q_s K_B}{Q_s K_A - Q_2} \quad \text{(23c)}$$

For the same operating conditions the ratio $(C_{bA2})/(C_{bB3}$ as a function of the adsorbent capacity loss (deactivation %) is shown Fig. 5.

It can be observed that for the adsorbent capacity decline higher than 3% the species A concentration plateau in zone 2 is higher than the concentration plateau of species B in zone 3 and *vice-versa*.

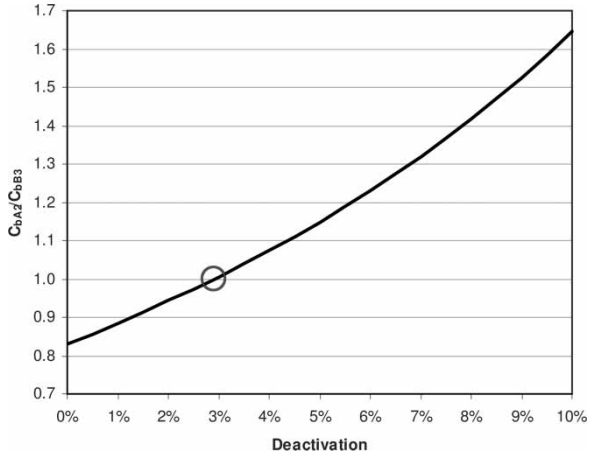

Figure 5. Concentration ratio $(C_{bA2})/(C_{bB3})$ in plateaus as a function of adsorbent deactivation (%), assuming the equilibrium theory.

Non-linear Isotherm Case

It is interesting to test the influence of the adsorbent capacity decrease on the SMB performances in the case of the non-linear isotherm, as for example the most common isotherm type in chiral separation: linear plus Langmuir isotherm:

$$q_i^* = m_i C_{bi} + \frac{Q_m b_i C_{bi}}{1 + \sum_{i=1}^{NC} b_k C_{bk}} \tag{24c}$$

it can be assumed that for a constant feed concentration, the adsorbed concentration decline results from the decrease of the maximum adsorption capacity (Q_m). Of course ageing can also affect the particle porosity and diffusivity. Nevertheless, only the reduction of the maximum adsorption capacity will be considered in this study:

$$Q_m = Q_m^0 \cdot f(t) \tag{24c}$$

where Q_m^0 represents the initial adsorption isotherm constant and $f(t)$ is a law of the adsorbent ageing as a function of time.

The enantiomer separation presented by Rodrigues and Pais (60) is considered as a case study for SMB binary separation with non-linear adsorption isotherms. The interstitial velocity ratios values (γ_j^* or γ_j) for sections 1 and 4, were kept constant and far from the critical values calculated by the equilibrium theory, needed for complete solid and eluent regeneration in section 4 and 1, respectively. For the sections 2 and 3 the interstitial velocity ratios were taken from the analysis presented by Rodrigues and Pais based on the ($\gamma_3 \times \gamma_2$) separation region for a 99.0% purity criterion with mass transfer coefficient of $k_{LDF} = 0.33\ s^{-1}$. The summary of all operating conditions and model parameters is presented in Tables 4 and 5.

Table 4. SMB unit characteristic parameters (60)

Model parameters	SMB columns
Pe = 1000	$N_c = 8$ $n_j = [2\ 2\ 2\ 2]$
$\varepsilon_b = 0.4$;	$L_c = 9.9$ cm
$R_p = 2.25 \times 10^{-5}$ m	$d_c = 2.6$ cm
	Classic SMB operating conditions
$k_{LDF} = 0.33\ s^{-1}$	$C_A^F = 5\ g \cdot l^{-1}$; $C_B^F = 5\ g \cdot l^{-1}$ $t_s = 198$ s;
	$Q_E = 25.038\ ml \cdot min^{-1}$; $Q_X = 17.980\ ml \cdot min^{-1}$;
	$Q_F = 0.956\ ml \cdot min^{-1}$; $Q_R = 8.014\ ml \cdot min^{-1}$;
	$Q_4 = 17.790\ ml \cdot min^{-1}$.

Table 5. The SMB and equivalent TMB sections operating conditions

Real SMB	Equivalent TMB
$\gamma_j^* = [6.722\ 3.900\ 4.050\ 2.793]$	$\gamma_j = [5.722\ 2.900\ 3.050\ 1.793]$
$Q_j^* = [42.828\ 24.848\ 25.804\ 17.790]$ ml · min^{-1}	$Q_j = [36.458\ 18.477\ 19.433\ 11.420]$ ml · min^{-1}
	$Q_s = 9.557$ ml · min^{-1}

The linear plus Langmuir isotherms in terms of retained concentration in the particles for both species are:

$$q_{Ac}^* = 1.35C_{bAc} + \frac{7.32 \cdot 0.163C_{bAc}}{1 + 0.163C_{bAc} + 0.087C_{bBc}} \tag{25a}$$

$$q_{Bc}^* = 1.35C_{bBc} + \frac{7.32 \cdot 0.087C_{bBc}}{1 + 0.163C_{bAc} + 0.087C_{bBc}} \tag{25b}$$

with q_{ij}^* in $g \cdot L_{adsorbent}^{-1}$ and C_{bij} in $g \cdot L^{-1}$

Keeping the same operating parameters and running simulations for different adsorbent ageing rates, it is possible to observe how internal concentration profiles (Fig. 6) and SMB performance parameters (Table 6) are affected by the adsorbent capacity decline.

The concentration profiles moved to the right as already observed for the case of linear adsorption isotherms. Again the raffinate purity will decrease for the higher adsorbent capacity decrease.

Considering the equilibrium theory for non-linear systems it must be taken into account that the separation region is no more a rectangular triangle as shown before for the linear case, but has a "triangle shaped form" (52), here, and for simplicity, without the curved lines (Fig. 7).

As can be perceived from Fig. 7, and was observed before for the linear isotherm case, the separation region moves downwards in the ($\gamma_2 \times \gamma_3$) plan when the adsorbent capacity decline increases.

Increase of Mass Transfer Resistances due to Adsorbent Ageing Problems

The influence of the increase of mass transfer resistances on the SMB performance will be studied by analysing the consequences of k_{LDF} value decrease:

$$k_{LDF} = k_{LDF}^0 \cdot g(t) \tag{26}$$

where k_{LDF}^0 represents the initial mass transfer coefficient and *g(t)* a general law of the mass transfer resistance increase due to adsorbent ageing problem as a function of time.

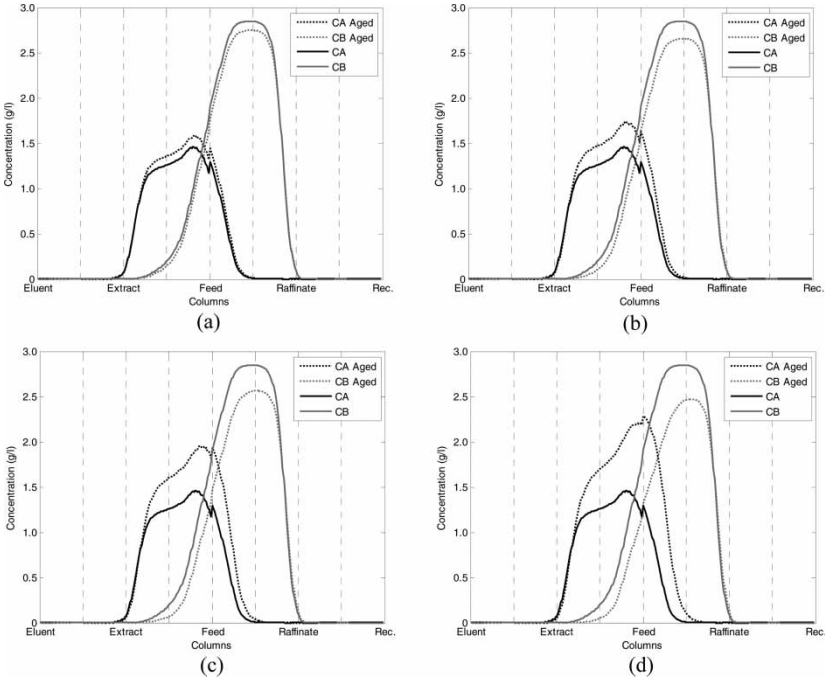

Figure 6. SMB concentration profiles of the enantiomers as result of aged adsorbent (a) $Q = 7.17$ (less 2%), (b) $Q = 7.03$ (less 4%), (c) $Q = 6.88$ (less 6%) and (d) $Q = 6.73$ (less 8%), at half time switch in the CSS.

Linear Isotherms Case

Various adsorbent ageing levels, due to the increase of the mass transfer limitation, have been simulated by reducing the mass transfer coefficient values for both fructose and glucose by 10, 20, 30, and 40% of its initial value, keeping the same operating conditions as those presented in Tables 1 and 2. The

Table 6. SMB performance parameters values for different levels of adsorbent deactivation: 2, 4, 6 and 8% (adsorbent capacity decrease: $Q = 7.17$, $Q = 7.03$, $Q = 6.88$ and $Q = 6.73$, respectively)

Deactivation (%)	PUX^A (%)	PUR^B (%)	REX^A (%)	RER^B (%)
0	99.0	100.0	100.0	99.0
2	99.4	100.0	100.0	99.4
4	99.6	100.0	100.0	99.7
6	99.8	99.7	99.6	99.9
8	99.9	99.8	99.4	100.0

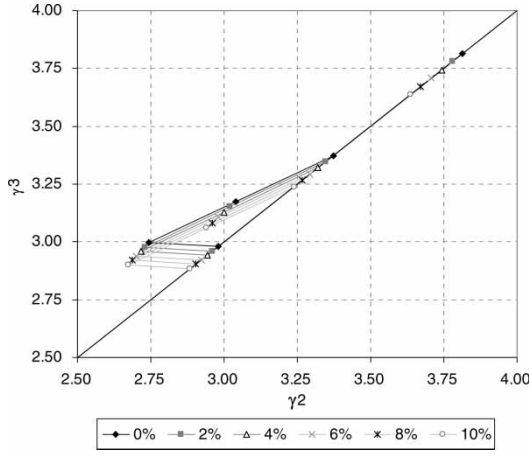

Figure 7. Nonlinear separation region for the studied enantiomer separation, different ageing adsorbent rates (0%, 2%, 4%, 6%, 8% and 10% adsorbent capacity decrease).

concentration profiles at half switching time in the CSS and SMB performance parameters are presented in Fig. 8 and Table 7, respectively.

As can be observed from Fig. 8, with the increase of mass transfer limitation the concentration plateaus of both species remain unchanged, but the concentration profiles become more dispersed, leading to SMB products contamination and decline of the product purities and recoveries (see Table 7).

Non-Linear Isotherms Case

The same procedure is now applied for the non-linear case, considering 10, 20, 30, and 40% decrease of k_{LDF} for both species; the remaining operating conditions are kept constant as those presented in Tables 4 and 5. The effect of different levels of mass transfer resistance increase on the enantiomers concentration profiles at half switching time in the CSS and SMB performances are presented in Fig. 9 and Table 8, respectively.

Again, from Fig. 9 and Table 8 it can be noted that when mass transfer resistances increase, due to adsorbent ageing, lower purity and recovery were obtained, either for the more retained product in the extract or for the less retained one in the raffinate. In this case, as in the case of linear isotherm, the plateaus remain unchanged, but the concentration profiles become more dispersed, the contaminating fronts have been stretched leading to SMB products contamination.

At this point it is interesting to observe that the adsorbent capacity decline or mass transfer resistance increase, have different influence on the concentration profiles in certain zones. Both ageing consequences led to similar behaviors on concentration profiles for the more retained component in section 3 and the less retained species in section 4. Namely, the contaminating

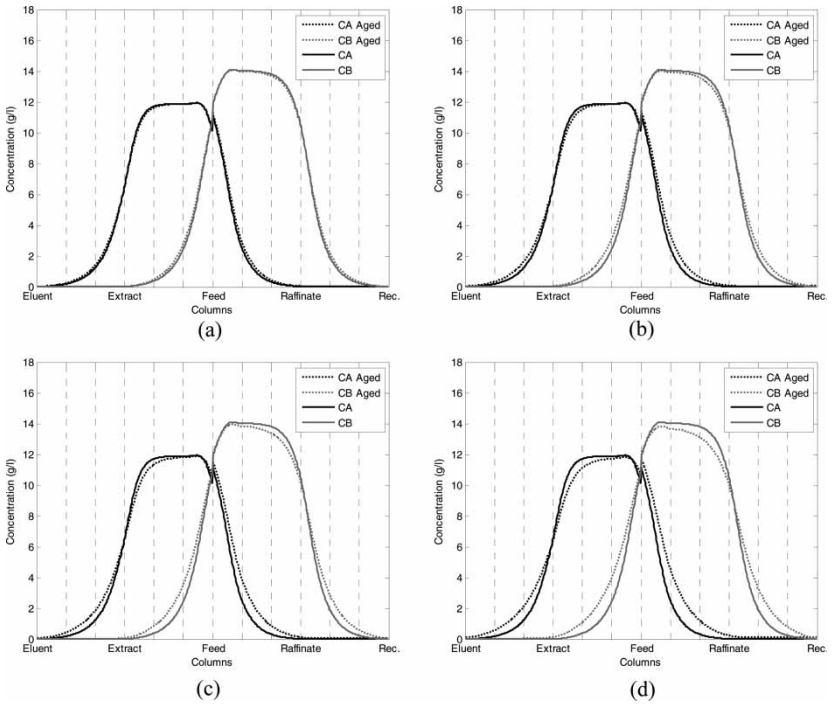

Figure 8. SMB concentration profiles of fructose (*A*) and glucose (*B*) as result of mass transfer coefficient decrease (a) $k_{LDF} = 0.09\text{s}^{-1}$ (less 10%), (b) $k_{LDF} = 0.08\text{s}^{-1}$ (less 20%), (c) $k_{LDF} = 0.07\text{s}^{-1}$ (less 30%) and (d) $k_{LDF} = 0.06\text{s}^{-1}$ (less 40%), at half time switch in the CSS).

or collection fronts in sections 3 and 4 have moved to the right. Therefore, if the two ageing factors are present at the same time it is difficult to know which one is the dominant. On the other hand, the changes in concentration profiles as a result of adsorbent capacity decline and mass transfer resistance increase are different in sections 1 and 2; in fact, with the adsorbent capacity decline,

Table 7. SMB performance for different levels of adsorbent deactivation: 10, 20, 30 and 40% (adsorbent mass transfer resistance increase: $k_{LDF} = 0.09\text{s}^{-1}$, $k_{LDF} = 0.08\text{s}^{-1}$, $k_{LDF} = 0.07\text{s}^{-1}$ and $k_{LDF} = 0.06\text{s}^{-1}$, respectively)

Deactivation (%)	PUX^{A} (%)	PUR^{B} (%)	REX^{A} (%)	RER^{B} (%)
0	99.5	99.6	99.6	99.5
10	99.3	99.4	99.4	99.3
20	98.9	99.0	99.0	98.9
30	98.2	98.4	98.4	98.2
40	97.2	97.3	97.3	97.2

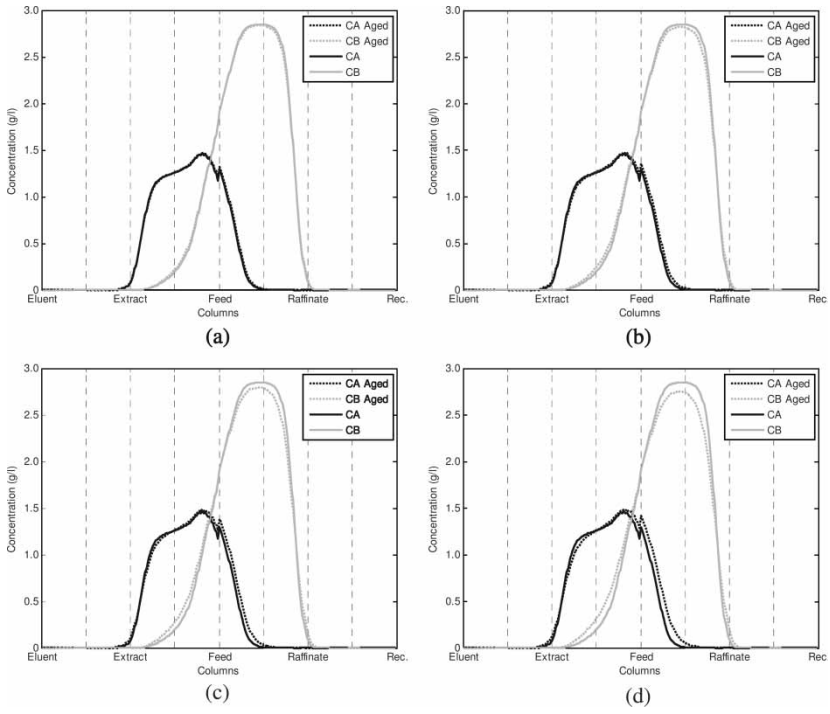

Figure 9. SMB concentration profiles for enantiomers separation with increasing mass transfer resistance (a) $k_{LDF} = 0.30\,s^{-1}$ (less 10%), (b) $k_{LDF} = 0.26\,s^{-1}$ (less 20%), (c) $k_{LDF} = 0.23\,s^{-1}$ (less 30%) and (d) $k_{LDF} = 0.20\,s^{-1}$ (less 40%), at half time switch in the CSS.

the mentioned fronts are moving to the right while in the case of ageing leading to mass transfer resistances increase, the same fronts move to the left. So, the movement of fronts in section 1 and 2 can be used for the diagnosis of the dominant ageing factor.

Table 8. SMB performance parameters for different levels of adsorbent deactivation: 10, 20, 30, and 40% (adsorbent mass transfer resistance increase: $k_{LDF} = 0.30s^{-1}$, $k_{LDF} = 0.26s^{-1}$, $k_{LDF} = 0.23s^{-1}$ and $k_{LDF} = 0.20s^{-1}$, respectively)

Deactivation (%)	PUX^A (%)	PUR^B (%)	REX^A (%)	RER^B (%)
0	99.0	100.0	100.0	99.0
10	98.7	100.0	100.0	98.7
20	98.3	100.0	100.0	98.4
30	97.8	100.0	99.9	97.9
40	97.0	99.9	99.8	97.1

CORRECTIVE STRATEGIES

Adsorbent Capacity Decline Due to Adsorbent Deactivation

From Figs 3. and 7, it can be concluded that to have similar SMB performance with aged adsorbent as those with fresh absorbent, the γ_j operating parameters should be decreased, keeping the same relative distance to the respective constraints (triangle borders).

Keeping the same inlet and outlet flow rates, two straightforward corrective strategies to decrease the γ_j values are possible:

i. decrease the SMB switching time (increase of the solid velocity); and
ii. decrease the recycle flow rate (Q_4).

The paths of these corrective measurements presented in (γ_2, γ_3) plane are shown in Fig. 10. The switching time corrective path (c), follows the adsorbent ageing pathway, (see the vertex line in Figure 10). On the other hand, the recycle flow rate corrective measurement lead to corrective path (p) parallel to the $\gamma_2 = \gamma_3$ line in the separation zone plan.

Also, it is quite simple to understand that the adsorbent deactivation can be compared to the decrease of the "active" solid flow rate and a simple way to compensate it is to increase the solid flow rate.

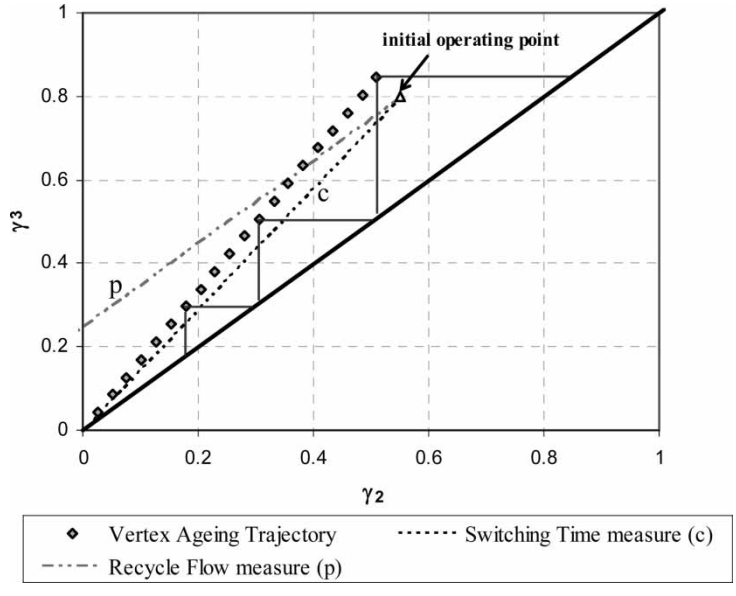

Figure 10. Comparison between two possible corrective measures to adsorbent capacity decline, the switching time decrease (solid flow rate increase, path (c)) and internal flow rate decrease, path (p).

A better visualization of this assumption can be obtained by reformulation of Fig. 2, presenting the equilibrium theory constraints in terms of fluid phase flow rates. In Fig. 11 the separation zone is presented in (Q_2 vs. Q_3) plane and the regeneration zone is presented in (Q_1 vs. Q_4) plane. The separation region constraints are now $K_BQ_s < Q_2 < Q_3 < K_AQ_s$; the constraints for the regeneration zones are now $Q_4 < K_BQ_s$ and $Q_1 > K_AQ_s$.

At this stage, it becomes quite easy to understand that a simple and direct corrective measure of the adsorbent capacity decline in the SMB units operating under equilibrium conditions could be the decrease of the SMB switching time (increase of the solid flow rate). Although, in the SMB separations where mass transfer limitations are present, the solution of the adsorbent aging problem related to the adsorption capacity decline will not be as simple as can be observed from Fig. 11.

The separation regions for the fructose/glucose SMB separation (56) for different product purities requirements calculated with the LDF-TMB model are presented in Fig. 12 for a fresh adsorbent.

In this case, the separation region is not a rectangular triangle for a given purity value as stated by the Equilibrium Theory, but has a rounded shape, similar to the one mentioned in the separation volume methodology (61). This rounded shape is also a function of the solid flow rate. Namely, when higher values of the solid flow rates are used the mass transfer resistances become more important and the deviation from the separation regions defined by the Equilibrium Theory becomes more significant. In fact, the solid residence time becomes shorter and the ratio between the switching time (solid residence time) and the τ_p (intraparticle mass transfer time

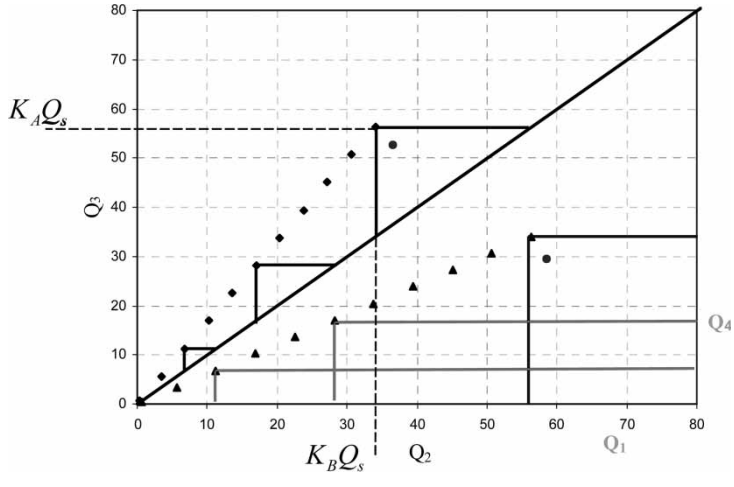

Figure 11. Separation and regeneration zones represented in (Q_2,Q_3) and (Q_1,Q_4) plane, respectively: black dots are vertexes for different solid flow rates, grey dots are possible operating point ($Q_s = 100\ \text{ml} \cdot \text{min}^{-1}$).

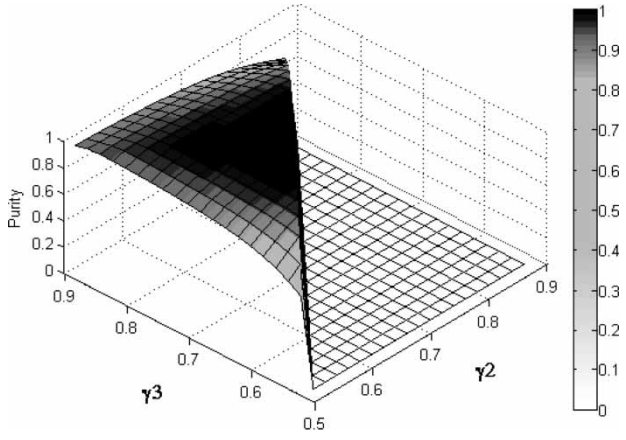

Figure 12. Separation zone for different product purities requirements for the case of glucose/fructose SMB separation (56), $Q_s = 20.93\ \text{ml} \cdot \text{min}^{-1}$.

constant $\tau_p = (1)/(k_{LDF})$ decreases. Therefore the corrective strategies to be studied will take into account the mass transfer limitations described by the TMB model with LDF.

Initially, the SMB(TMB) inlet/outlet flow rates $[Q_D \ Q_X \ Q_F \ Q_R] = [8.23 \quad 5.62 \quad 1.28 \quad 3.89]\ \text{ml} \cdot \text{min}^{-1}$ and the zone flow rates will be kept constant.

The analysis on the corrective measure is done by applying a one degree of freedom (DOF) analysis, decreasing the operating parameters γ_j, varying Q_s and observing the performance parameters evolution for different values of adsorbent deactivation.

By increasing the solid flux Q_s (decrease of switching time), it is possible as a first approach, to reach the new optimum operating conditions obtaining performance parameters near to those predicted when using fresh adsorbent. Consequently, it becomes interesting to observe the performance parameters dependence on the switching time at different levels of deactivation, presented in Fig. 13. The influence on the productivity parameters is similar to the recovery, as stated in Eq. (19c).

Anyhow, the adsorbent capacity decline leads to a decrease of the SMB performance, even when the optimum switching time is used for the compensation at each degree of adsorbent ageing. However, there is a narrow plateau (in the range between 0% and $+/-30\%$ of adsorbent capacity decline) where the variation of the time switch helps in the ageing problem compensation, as shown in Fig. 14.

Mass Transfer Resistances Increase Due to Adsorbent Deactivation

The TMB and SMB mass balances model equations have been rewritten considering the alternative k_{LDF} formulation defined by Eq. (18).

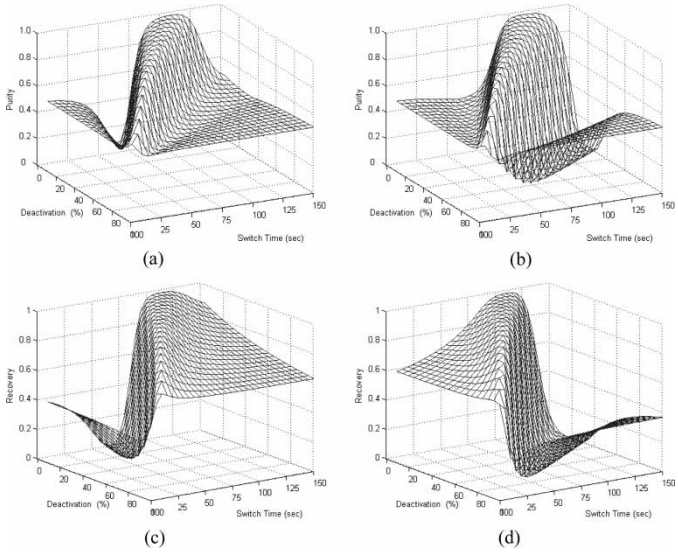

Figure 13. Effect of switching time analysis for different values of adsorbent ageing deactivation values (percentage of adsorbent capacity decrease), in the SMB performance parameters, (a) A purity in the extract, (b) B purity in the raffinate, (c) A recovery in the extract and (d) B recovery in the raffinate, linear isotherms case from Leão and Rodrigues (56).

In the TMB model steady state operation $((\partial C_{bij}/\partial\theta) = 0 \;\; (\partial\langle q_{ij}\rangle)/(\partial\theta) = 0)$, is also assumed: the bulk fluid mass balance,

$$0 = -\frac{dC_{bij}}{dx} - \frac{(1 - \varepsilon_b)}{\varepsilon_b}\frac{k_{LDF}}{u_j}L_j(q_{ij}^{*} - \langle q_{ij}\rangle) \tag{27a}$$

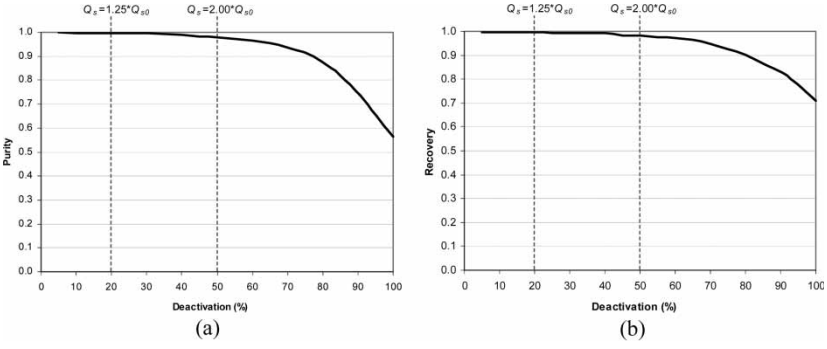

Figure 14. Solid flow rates optimum values, leading to the highest possible purity for different adsorbent ageing deactivation values (percentage of adsorbent capacity decrease) (a), and recovery (b). The Q_s equivalent solid flow rate and Q_{s0} is the solid flow rate for fresh adsorbent).

the "solid phase" mass balance,

$$0 = \frac{d\langle q_{ij}\rangle}{dx} + \frac{k_{LDF}}{u_s} L_j (q^*_{ij} - \langle q_{ij}\rangle) \tag{27b}$$

In the transient state SMB model the mass balances equations now are: the bulk fluid mass balance,

$$\frac{\partial C_{bij}}{\partial \theta} = -\frac{u^*_j t_s}{L_c}\frac{\partial C_{bij}}{\partial x^*} - \frac{(1 - \varepsilon_b)}{\varepsilon_b} k^*_{LDF} t_s (q^*_{ij} - \langle q_{ij}\rangle) \tag{28a}$$

the "solid phase" mass balance,

$$\frac{\partial \langle q_{ij}\rangle}{\partial \theta} = k^*_{LDF} t_s (q^*_{ij} - \langle q_{ij}\rangle) \tag{28b}$$

It can be easily understood that a k_{LDF} (or k^*_{LDF}) decrease can be compensated by a same amplitude decrease on u_j (or u^*_j) and u_s (or t_s increase) values, and therefore, maintaining the unit purity and recovery values. Nevertheless, this compensation measure leads to a productivity value decrease, with the same amplitude as for the mass transfer coefficient decrease. For example, if the mass transfer coefficient decreases 10% the productivity will also decrease around 10%. This strategy will maintain the same dimensionless operating parameters γ_j (or γ^*_j), since u_j (or u^*_j) and u_s values decrease is done by the same factor, equal to that of k_{LDF} (or k^*_{LDF}). For the corrected values of u_j (or u^*_j) and u_s (or t_s), the separation region ($\gamma_2 \times \gamma_3$) will be the same as the one obtained when new adsorbent is used.

With this short cut strategy it is impossible to maintain the same productivity value as the one calculated for a fresh adsorbent unit, but it is easy to understand and operate the unit keeping the purity requirements. A more complete analysis would be necessary to compensate the mass transfer resistance increase and at same time guarantee maximum productivity; however, it would require a considerable effort considering all operating conditions, solid and all liquid flow rates, and therefore, a more complex compensating measure.

The calculation effort will be therefore almost the same as designing a new unit. With the re-optimization, new values of the solid and liquid flow rates will be established in a manner like mass transfer resistances increase compensation without losing too much in unit productivity, but losing in other performance parameters, either the extract purity and raffinate recovery or *vice-versa*.

Once again the glucose/fructose SMB separation (56) is used as a case study in this analysis. The concentration profiles and unit performances obtained for the case simulation presented in Fig. 8b, when adsorbent mass transfer resistances increases for 20% and 20% decrease correction is applied for both u^*_j as u_s (time switch increase), are presented in Fig. 15 and Table 9, respectively.

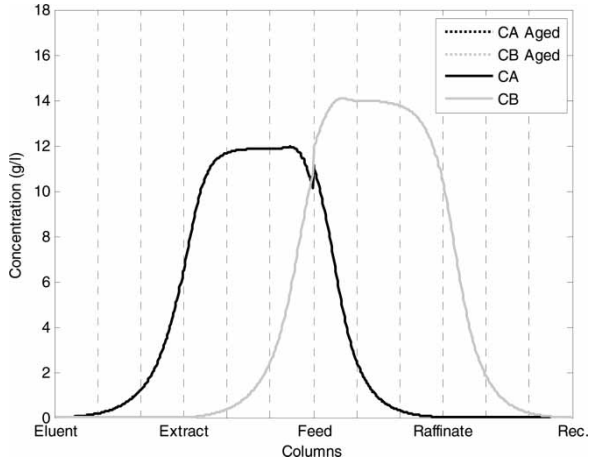

Figure 15. Concentration profiles for fresh adsorbent and 20% deactivation with mass transfer compensation (both profiles are coincident): linear adsorption isotherms.

As can be observed from Fig. 15 and Table 9, with the application of the proposed straightforward compensating measure is was possible to obtain the same concentration profiles as the ones obtained when the adsorbent was fresh, keeping the same product purity and recovery performances. As was expected the productivity drops for 20%.

UNIT REARRANGEMENT

The strategies presented above are dynamic and can be applied continuously if the ageing law is well know. In the case of adsorbent capacity decline some sections have improved their function (see Fig. 4), namely sections 1 and 2, where the length needed now for solid regeneration and extract purification is shorter than the one needed when the adsorbent was new. The opposite is observed for sections 3 and 4. A simple corrective measure to the adsorbent capacity decline due to ageing could be the utilization of the "non-used" columns from sections 1 and 2 in sections 3 and 4, where they are needed

Table 9. Performance parameters for fresh adsorbent, 20% deactivation by mass transfer resistance increase and compensated case: linear adsorption isotherms

Deactivation (%)	PUX^A (%)	PUR^B (%)	REX^A (%)	RER^B (%)
0	99.5	99.6	99.6	99.5
20	98.9	99.0	99.0	98.9
20 (corrected)	99.5	99.6	99.6	99.5

most. Nevertheless, the practical application of the SMB columns distribution re-arrangement would be difficult to implement, since this corrective measurement would require more problematic unit stabilization (the achievement of a novel cyclic steady-state). It would be possible to realize the SMB columns relocation in the cases where the adsorbent capacity decline law is smooth, namely, a long time is required to loose the adsorbent capacity and the unit has a large number of columns, then it would be possible to implement it. Otherwise, the only way for its implementation is to use variable switch time values in Varicol strategy. Applying the variable time switches in the Varicol operational mode would be possible to change the number of columns per section as corrective measure for the adsorbent ageing problem, for example passing from [2 2 1 1] configuration to [1.5 1.5 1.5 1.5] and [1 1 2 2], etc.

This corrective strategy will be analysed for the SMB enantiomer separation studied by Pais and Rodrigues (62) where the adsorption isotherms measured at 25°C are represented by the linear + Langmuir competitive model:

$$C_{sAc} = 0.90C_{pAc} + \frac{7.32 \cdot 0.163C_{pAc}}{1 + 0.163C_{pAc} + 0.087C_{pBc}} \tag{29a}$$

$$C_{sBc} = 0.90C_{pBc} + \frac{7.32 \cdot 0.087C_{pBc}}{1 + 0.163C_{pAc} + 0.087C_{pBc}} \tag{29b}$$

with C_{sic} in $g \cdot L^{-1}_{adsorbent}$ and C_{pic} in $g \cdot L^{-1}$ or the equivalent isotherms in terms of retained concentration in the particles presented by Eq. (30).

The SMB unit characteristics parameters are presented in Table 10 and Table 11.

This case study is simulated by the SMB model for the corresponding [1 1.5 1.5 1] Varicol configuration and [1 1.75 1.25 1] Varicol configuration, in the case of fresh adsorbent. When the [1 1.75 1.25 1] Varicol configuration used in all concentration fronts will move to the left, as presented in Fig. 16.

Table 10. SMB characteristic parameters and operating conditions from (62)

Model parameters	SMB columns
Pe = 1600	$N_c = 5$
$\varepsilon_b = 0.4$; $\varepsilon_p = 0.45$	$L_c = 15.84$ cm
$R_p = 2.25 \times 10^{-5}$ m	$d_c = 2.6$ cm
	SMB operating conditions
$k_{LDF} = 0.4\ s^{-1}$	$C^F_A = 5\ g \cdot l^{-1}$; $C^F_B = 5\ g \cdot l^{-1}$ $t_s = 317$ s; $Q_s = 9.54$ ml · min^{-1} $Q_E = 25.02$ ml · min^{-1}; $Q_X = 17.34$ ml · min^{-1}; $Q_F = 0.66$ ml · min^{-1}; $Q_R = 8.34$ ml · min^{-1}; $Q_4 = 17.76$ ml · min^{-1}.

Table 11. SMB and equivalent TMB section operating conditions

Real SMB	Equivalent TMB
$\gamma_j^* = [6.722\ 4.000\ 4.100\ 2.793]$	$\gamma_j = [5.722\ 3.000\ 3.100\ 1.793]$
$Q_j^* = [42.78\ 25.44\ 26.10\ 17.76]$ $\text{ml} \cdot \text{min}^{-1}$	$Q_j = [36.42\ 19.08\ 19.74\ 11.40]$ $\text{ml} \cdot \text{min}^{-1}$

This is important since the adsorbent ageing problem (capacity decline) will do the opposite, the "problematic" containing fronts will move to right. Figure 17 shows the [1 1.5 1.5 1] Varicol simulation values for the example described by the adsorption equilibrium for the aged adsorbent:

$$q_{Aj}^* = 1.31C_{bAj} + \frac{7 \cdot 0.163C_{bAj}}{1 + 0.163C_{bAj} + 0.087C_{bBj}} \tag{30a}$$

$$q_{Bj}^* = 1.31C_{bBj} + \frac{7 \cdot 0.087C_{bBj}}{1 + 0.163C_{bAj} + 0.087C_{bBj}} \tag{30b}$$

In Eq. (30) the adsorbent capacity was decreased in the Langmuir part as in the linear part. The initial adsorbent Eq. (29) and the aged ones Eq. (30) simulated results for the [1 1.5 1.5 1] Varicol strategy is presented in Fig. 17.

Similarly to the analysis of the standard SMB configuration, the concentration profiles with aged adsorbent, appear to the right from those obtained with fresh adsorbent. Also, the enantiomer concentration plateau has

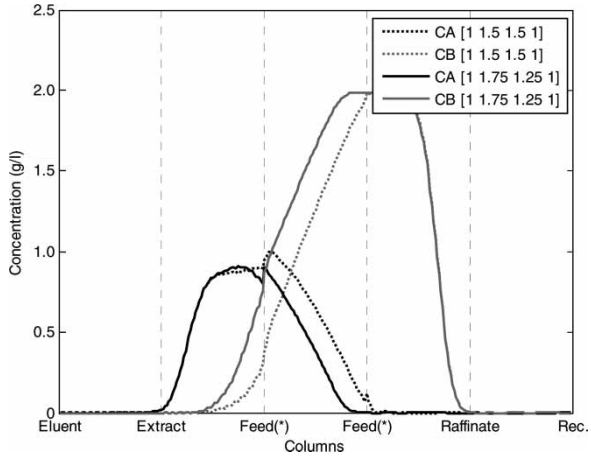

Figure 16. Enantiomers concentration profiles for [1 1.5 1.5 1] and [1 1.75 1.25 1] Varicol configuration, at half switching time in CSS (fresh adsorbent).

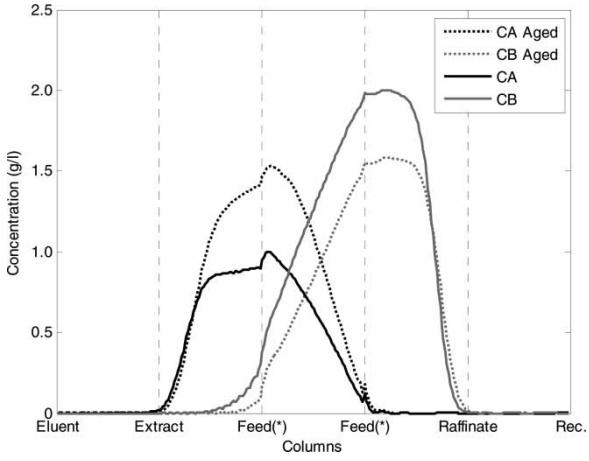

Figure 17. Concentration profiles for [1 1.5 1.5 1] Varicol configuration: new adsorbent-solid line; aged adsorbent-dashed line, at half switching time in CSS.

increased in section 2 and decreased in section 3, as result of the adsorbent capacity decline.

In order to avoid the raffinate contamination, a new [1 1.75 1.25 1] Varicol configuration has been tested for the case of aged adsorbent. In Fig. 18, the concentration profiles in the case of aged adsorbent Eq. (30) for [1 1.5 1.5 1] and [1 1.75 1.25 1] Varicol configurations are presented.

In this case, only by changing the feed strategy (during 0.75 of switch time feed is in column 3 inlet and remaining time in the column 4 inlet),

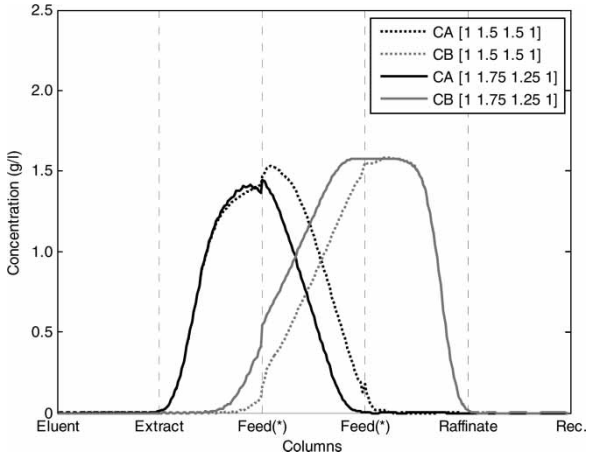

Figure 18. Enantiomers concentration profiles for aged adsorbent: [1 1.5 1.5 1] Varicol configuration–dashed line and [1 1.75 1.25 1] Varicol configuration–solid line, at half time switch in CSS.

the problem caused by the adsorbent ageing was almost compensated. A more detailed study of this strategy, including optimization and considering also deactivation with the increase of the mass transfer resistance, might reveal more potential in the use of variable time switches (variable columns distribution) as a compensating measure to ageing problems, and therefore shall be a matter of further studies.

CONCLUSIONS

The consequences of adsorbent deactivation described by adsorbent capacity decline or mass transfer resistances increase are presented. The operation of SMB units has been studied for two different systems:

i. linear isotherms case and ageing by adsorbent capacity decline and increased mass transfer resistance;
ii. non-linear isotherms case (linear + Langmuir isotherms) for ageing with adsorbent capacity decline only.

The systems were modelled by the SMB model with the LDF approach and solved with the commercial gPROMS package from Process System Enterprise. In both cases it has been observed that there is a decrease of purities/recoveries and therefore unit productivity as a result of adsorbent ageing.

Corrective strategies to the ageing problem were developed:

i. To compensate the adsorbent capacity decline it has been found that decreasing switching time it is possible to maintain the initial SMB performance, until the limit when mass transfer limitations become important due to short solid residence time;
ii. To compensate the mass transfer resistances increase it has been shown that the decrease of solid and internal flow rates would lead to the same purity and recovery; however, the productivity will decrease;
iii. Also, it was shown how a variable switch times use in the non-conventional application of Varicol strategy could compensate the loss of adsorbent capacity.

NOTATION

C_b	bulk fluid phase concentration $\text{mol} \cdot \text{m}^{-3}$
C^F	feed concentration $\text{mol} \cdot \text{m}^{-3}$
$<q_{ij}>$	average particle concentration $\text{mol} \cdot \text{m}_{\text{solid}}^{-3}$
D_b	axial dispersion coefficient $\text{m}^2 \cdot \text{s}^{-1}$
D_{pe}	particle effective diffusivity $\text{m}^2 \cdot \text{s}^{-1}$
d_c	Column diameter m
K	linear adsorption isotherm Henry constant $\text{m}^3 \cdot \text{kg}^{-1}$

L_c	column axial length m
L_j	section axial length m
n_j	number of columns per section
Nc	total number of components
Pe	Peclet number
Prx	unit productivity $g \cdot (s \cdot m^3_{solid})^{-1}$
Pux	purity %
Q	fluid/solid flow rate $m^3 \cdot s^{-1}$
q^*	solid retained concentration $mol \cdot m^{-3}_{solid}$
Rex	recovery %
R_p	particle radius m
t	time variable s
t_j	bulk fluid space time s
t_s	solid space time (switching time) s
u_j	interstitial fluid velocity in j section $m \cdot s^{-1}$
u_s	solid interstitial counter-current velocity $m \cdot s^{-1}$
x	dimensionless axial column coordinate
z	axial column coordinate m

Greek Letters

α	dimensionless mass transfer resistance parameter
γ	ration between fluid and solid interstitial velocities
ε_b	bed porosity
ε_p	particle porosity
θ	time normalise by the switching time

Indexes

*	in the SMB model
A	more retained species
B	less retained species
b	bulk
p	particle
s	solid
c	column
i	chemical species
j	SMB/TMB section
E	eluent stream
F	feed stream
R	raffinate stream
X	extract stream

Abbreviations

AE	Algebraic equations
CSS	Cyclic steady state

DAE	Differential-Algebraic equations
LDF	Linear driving force
OCFEM	Orthogonal collocation in finite elements method
ODE	Ordinary differential equations
PDAE	Partial differential algebraic equations
PDE	Partial differential equations
SMB	Simulated moving bed
TMB	True moving bed
LSC	Lower solvent consumption (point)

ACKNOWLEDGMENTS

Pedro Sá Gomes acknowledges the financial support from FCT "Fundação para a Ciência e a Tecnologia" (Ph.D. grant SFRH/BD/22103/2005), Ministry of Science and Technology of Portugal. Financial support through the project POCI/EQU/59296/2004 is gratefully acknowledged.

REFERENCES

1. Broughton, D.B. and Gerhold, C.G. (1961) Continuous Sorption Process Employing Fixed Bed of Sorbent and Moving Inlets and Outlets. US Patent No 2 985 589.
2. Broughton, D.B., Neuzil, R.W., Pharis, J.M., and Brearley, C.S. (1970) The Parex process for recovering paraxylene. *Chem. Eng. Progress*, 66: 70–75.
3. Ash, G., Barth, K., Hotier, G., Mank, L., and Renard, P. (1994) ELUXYL: A new paraxylene separation process rev. *Inst. Fr. Petr.*, 49 (05): 541–549.
4. Pavone, D. and Hotier, G. (2000) System approach modelling applied to the eluxyl process. *Revue IFP.*, 55: 437.
5. Nicoud, R.M. (1999) The separation of optical isomers by simulated moving bed chromatography. *Pharm. Tech. Europe*, 11: 28–34.
6. Nicoud, R.M. (1999) The separation of optical isomers by simulated moving bed chromatography. *Pharm. Tech. Europe*, 11: 36–44.
7. Adam, P.R., Nicoud, R.M., Bailly, M., and Ludemann-Hombourger, O. (2000) Process and device for separation with variable-length. U.S. Patent No 6 136 198.
8. Ludemman-Hombouger, O., Nicoud, R.M., and Bailly, M. (2000) The "Varicol" Process: a new multicolumn continuous chromatographic process. *Separation Science and Technology*, 35 (12): 1829–1862.
9. Zhang, Z., Mazzotti, M., and Morbidelli, M. (2003) Powerfeed operation of simulated moving bed units: changing the flow-rates during the switching interval. *Journal of Chromatography A*, 1006: 87–99.
10. Schramm, H., Kaspereit, M., Kienle, A., and Seidel-Morgenstern, A. (2002) Improving simulated moving bed processes by cyclic modulation of the feed concentration. *Chem. Eng. Tech.*, 25 (12): 1151–1155.
11. Schramm, H., Kaspereit, M., Kienle, A., and Seidel-Morgenstern, A. (2003) Simulated moving bed process with a cyclic modulation of the feed concentration. *Journal of Chromatography A*, 1006: 77–86.

12. Sá Gomes, P. and Rodrigues, A.E. (2007) Outlet Streams Swing (OSS) and MultiFeed (MF) operation of simulated moving beds. *Separation Science and Technolog,y*, 42: 223–252.
13. Kim, J.K., Abunasser, N., and Wankat, P. (2005) Use of Two feeds in simulated moving beds for binary separation. *Korean J. Chem. Eng.*, 22 (4): 619–627.
14. Hur, J.S. and Wankat, P.C. (2005) New design of simulated moving bed (SMB) for ternary separations. *Ind. Eng. Chem. Res.*, 44: 1906–1913.
15. Hur, J.S. and Wankat, P.C. (2006) Two-zone SMB/chromatography for center-cut separation from ternary mixtures: linear isotherm sytems. *Ind. Eng. Chem. Res.*, 45: 1426–1433.
16. Mata, V.G. and Rodrigues, A.E. (2001) Separation of ternary mixtures by pseudo-simulated moving bed chromatography. *J. Chromatography A*, 939: 23–40.
17. Borges da Silva, E.A. and Rodrigues, A.E. (2006) Continuous chromatographic separation of multicomponent mixtures using JO technology. *AIChE Journal*, 52: 3794–3812.
18. Silva, V.M.T.M. and Rodrigues, A.E. (2005) Novel process for diethylacetal synthesis. *AIChE Journal*, 51: 2752–2768.
19. Rodrigues, A.E. and Silva, V.M.T.M. (2004). Processo Industrial de Produção de Acetais num Reactor Adsorptivo de Leito Móvel Simulado. Patent no. PT103123. also published as (2005) Industrial Process for Acetals Production in a Simulated Moving Bed Reactor Patent No. WO113476 A1.
20. Bartholomew, C.H. (2001) Mechanisms of catalyst deactivation. *Applied Catalysis: General*, 212: 17–60.
21. Denny, P.J. and Twigg, M.V. (1980) In Catalyst Deactivation 1980 *Stud. Surf. Sci. Catal.*; Delmon, B. and Froment, G.F. (eds.); Elsevier: Amsterdam, Vol. 6, p. 577.
22. Bartholomew, C.H. (1984) Catalyst deactivation. *Chem. Eng.*, 91 (23): 96–112.
23. Butt, J.B. (1984) In *Catalysis, Science and Technology*; Anderson, J.R. and Boudart, M. (eds.); Springer: New York, p.1.
24. Farrauto, R.J. and Bartholomew, C.H. (1997) *Fundamentals of Industrial Catalytic Processes*; Chapman & Hall, Kluver Academic Publishers: London, Chapter 5.
25. Figueiredo, J.L. (ed.), (1982) Progress in catalyst deactivation, *NATO Advanced Study Institute Series E,* Marunus Nijhoff: Boston.
26. Hughes, R. (1984) *Deactivation of Catalysts*; Academic Press: London, Chapter 8.
27. Oudar, J. and Wise, H. (1985) *Deactivation and Poisoning of Catalysts*; Marcel Dekker: New York.
28. Butt, J.B. and Peterson, E.E. (1988) *Activation, Deactivation and Poisoning of Catalysts*; Academic Press: San Diego.
29. Delmon, B. and Forment, G.F. (1980) *Catalyst Deactivation, Stud. Surf. Sci. Catal.*; Elsevier: Amsterdam, Vol. 6.
30. Delmon, B. and Forment, G.F. (1987) *Catalyst Deactivation; Stud. Surf. Sci. Catal.*; Elsevier: Amsterdam, Vol. 34.
31. Delmon, B. and Forment, G.F. (1994) *Catalyst Deactivation; Stud. Surf. Sci. Catal.*; Elsevier: Amsterdam, Vol. 88.
32. Delmon, B. and and Forment, G.F. (1999) *Catalyst Deactivation Stud. Surf. Sci. Catal.*: Elsevier: Amsterdam, Vol. 126.
33. Bartholomew, C.H. and Butt, J.B. (1991) *Catalyst Deactivation, Stud. Surf. Sci. Catal.*; Elsevier: Amsterdam., Vol. 68.
34. Bartholomew, C.H. and Fuentes, G.A. (1997) *Catalyst Deactivation, Stud. Surf. Sci. Catal.*; Elsevier: Amsterdam., Vol. 111.

35. Sá Gomes, P., Minceva, M., and Rodrigues, A.E. (2006) Operation of Simulated Moving Bed in Presence of Adsorbent Ageing, 2006 AIChE Annual Meeting; paper 148c.
36. Minceva, M. and Rodrigues, A.E. (2002) Modelling and simulation of a simulated moving bed for the separation of *p*-Xylene. *Ind. Eng. Chem. Res.*, 41: 3454–3461.
37. Kohl, A. and Nielsen, R. (1997) *Gas Purification*; Gulf Publishing Company: Houston, Chap. 12, p. 1070.
38. Natarajan, S. and Lee, J.H. (2000) Repetitive model predictive control applied to a simulated moving bed chromatography systems. *Computers & Chemical Engineering*, 24: 1127–1133.
39. Abel, S., Erdem, G., Mazzotti, M., Morari, M., and Morbidelli, M. (2004) Optimizing control of simulated moving beds—linear isotherm. *Journal of Chromatography A*, 1033: 229–239.
40. Toumi, A. and Engell, A. (2004) Optimization based control of a reactive simulated moving bed process for glucose isomerization. *Chemical Engineering Science*, 59: 3777–3792.
41. Engell, S. (2007) Feedback control for optimal process operation. *Journal of Process Control*, article in Press.
42. Aida, T. and Silveston, P.L. (2005) *Cyclic Separating Reactors*; Blackwell Publishing: Oxford, Chap. 8, p. 162.
43. Pilliod, D.L., Randall, K.C., and Harding, E.M. (2006) A process for hydrocarbon conversion with on-line solid particulate material removal. WO Patent No 118739 A2.
44. Pilliod, D.L., Randall, K.C., and Harding, E.M. (2006). An adsorption process with on-line adsorbent removal. WO Patent No 118740 A1.
45. Frey, S.J., Sechrist, P.A., and Kauff, D.A. (2006) Fluid distribution apparatus. WO Patent No 055222 A1.
46. Minceva, M. and Rodrigues, A.E. (2005) Two-level optimization of an existing SMB for p-xylene separation. *Computers & Chemical Engineering*, 29: 2215–2228.
47. Storti, G., Mazzotti, M., Morbidelli, M., and Carrá, S. (1993) Robust design of binary counter-current adsorption separation processes. *AIChE Journal*, 39: 471–492.
48. DeVault, D. (1943) The Theory of chromatography. *J. Am. Chem. Soc.*, 65: 532–540.
49. Klein, G., Tondeur, D., and Vermeulen, T. (1967) multicomponent ion exchange in fixed beds: general proprieties of equilibrium systems. *Ind. Eng. Chem. Fundamentals*, 6 (3): 339–351.
50. Tondeur, D. and Klein, G. (1967) Constant-Separation-Factor equilibrium. *Ind. Eng. Chem. Fundamentals*, 6 (3): 351–361.
51. Helfferich, F.G. (1967) Multicomponent ion exchange in fixed beds: generalized equilibrium theory for systems with constant separation factors. *Ind. Eng. Chem. Fundamentals*, 6 (3): 362–364.
52. Helfferich, F. and Klein, G. (1970) *Multicomponent Chromatography*; Marcel Dekker: New York.
53. Rhee, H.-K., Aris, R., and Amundson, N.R. (1970) On the theory of multicomponent chromatography. *Phil. Trans. Roy. Soc. London A*, 267: 419–455.
54. Mazzotti, M., Storti, G., and Morbidelli, M. (1997) Optimal operation of simulated moving bed units for nonlinear chromatographic separations. *J. Chromatography A*, 769: 3–24.

55. Migliorini, C., Mazzotti, M., and Morbidelli, M. (2000) Design of simulated moving bed multicomponent separations: Langmuir systems. *Sep. and Pur. Tech.*, 20: 79–96.
56. Leão, C.P. and Rodrigues, A.E. (2004) *Computers and Chemical Engineering*, 28: 1725–1741.
57. Sá Gomes, P., Leão, C.P., and Rodrigues, A.E. (2007) Simulation of true moving bed adsorptive reactor: detailed particle model and linear driving force approximations. *Chemical Engineering Science*, 62: 1026–1041.
58. Glueckauf, E. (1955) Theory of chromatography part 10: Formula for diffusion into spheres and their application to chromatography. *Trans. Faraday Soc.*, 51: 1540–1551.
59. Ruthven, D.M. (1984) *Principles of Adsorption and Adsorption Processes*; John Wiley & Sons Inc.: New York, p. 243.
60. Rodrigues, A.E. and Pais, L.S. (2004) Design of SMB chiral separations units using concept of separation volume. *Sep. Sci. and Tech.*, 39: 245–270.
61. Azevedo, D.C. and Rodrigues, A.E. (1999) Design of a simulated moving bed in the presence of mass-transfer resistances. *AIChE Journal*, 45: 956–966.
62. Pais, L.S. and Rodrigues, A.E. (2003) Design of simulated moving bed and varicol processes for preparative separations with a low number of columns. *J. of Chromatography A*, 1006: 33–44.